

# Monitoring Of Concrete Bridge Using Robotic Total Station

Fong Kian Sin, Othman Zainon\*

Faculty of Built Environment and Surveying, Universiti Teknologi Malaysia 81310 Johor Bahru, Johor.

\*Corresponding author: othmanz.kl@utm.my

---

*Abstract* - Structural deformation monitoring is used to collect data on geometrical changes that occur within a structure. There are several techniques to carry out structural deformations monitoring surveys. The case study used in this the Sultan Idris Shah Bridge. It was constructed in 1907 and has required extensive maintenance on multiple occasions. This bridge is a vital transit route that is utilised daily by residents to move between Ipoh's old and modern towns. Due to these factors, including the bridge's age, traffic volume, and a strong water current beneath the bridge, it was anticipated that this structure would deform. Therefore, the purpose of this study is to explore the suitability of Robotic Total Station for monitoring concrete bridges deformation. The Sultan Idris Shah Bridge experienced deformation ranging from 1.3 cm to 4.2 cm, according to the findings. The study is based on two epochs of observation with a duration of three months. Monitoring points on the bridge's left side experienced deformation in a south-west direction, whereas monitoring points on the bridge's right-side experienced deformation in a north-west direction. The Robotic Total Station (RTS) employed in this study demonstrates that geometrical movement may be detected with centimetre-level accuracy. The findings propose a technique for future monitoring efforts that might be used to guide the application of RTS in structural monitoring.

*Keywords* - Structural, Deformation, Monitoring, bridge, Geometrical

©2021 Penerbit UTM Press. All rights reserved.

Article History: received 1 June 2021, accepted 19 July 2021, published 1 August 2021

*How to cite: Fong, KS and Zainon, O. (2021). Monitoring of Concrete Bridge Using Robotic Total Station. Journal of Advanced Geospatial and Science Technology. 1(1), 163-192.*

## **1. Introduction**

According to a research conducted by the Malaysia Public Works Department (JKR) in 1999, 17.92 percent of bridges are between the ages of 40 and 75, with 0.41 percent of bridges having been in service for more than 75 years (King and Public Work Department, 1999). The deterioration of material due to bridge ageing and increased traffic on the road has become a serious problem in many nations, compelling the government to spend more money on repairs, maintenance, and remediation on these ageing bridges on a regular basis (Palazzo et al., 2006). Bridge monitoring technology should be used on Malaysia's aged bridges to protect the safety of road users.

According to Masreta et al., (2021), more than 40% of bridges has exceeded 40 meters of the bridge pole height. According to Chen et al. (2020), the likelihood of pier damage increases with the flexibility of the ductility component of its failure. Therefore, according to Khodabandehlou, Pekcan, and Fadali (2019), the presence of damage and location and its type in a particular structural system can be identified by testing the actual vibration data collected from the bridge. Gaglione et al., (2018) state that general guidelines and considerations can be provided for the development of monitoring systems for bridge applications.

The purpose of structural deformation monitoring is to keep track of the structure's geometric displacement. The total station is well renowned for monitoring the structure's long-term movement (Cosser et al., 2003). However, due to the low sampling rate of the total station, it is difficult for the total station to monitor the local displacement of the structure accurately and precisely. The invention of modern Robotic Total Station (RTS) with higher accuracy and precision has improved the capability of a total station in monitoring surveys, especially with robotic motor, auto-tracking function, an auto-record function.

## **2. Engineering structure deformation**

Deformation will occur in engineering structures. Ogundare (2016) states that deformation can be described as changes that occurred to a deformable object, such as changes in shape, size, dimension, and position. Typically, the horizontal and vertical components of deformation are measured separately for better accuracy (Ogundare, 2016). Deformation, strain, load, stress, and groundwater pressure are all frequent parameters of a deformable object that are monitored, with deformation being the most prevalent. Deformation is a continuous process occurring on an object and affecting the whole object.

## ***2.1 Engineering structure deformation***

Structural deformation monitoring of engineering structures is constituted under a special branch of Geodesy Science (Erol, Erol, and Ayan, 2004). Structural deformation monitoring entailed the examination, measurement, and observation of a reference object or object point in or around the active area on a periodic basis, over an extended period of time, most often automatically or manually. The purpose of deformation analysis is to identify, localise, and model network point movements based on deformation measurements (Ogundare, 2016).

Structural deformation monitoring is used to gather data on the geometrical changes that occur at the structure under study. Additionally, a deformation monitoring survey is used to analyse an engineering structure and as a tool for interpreting the deformation physically (Abdullahi and Yelwa, 2016). There are several techniques for monitoring structural deformations. These are primarily classified into two categories: geodetic and non-geodetic techniques (Erol, Erol and Ayan, 2004). Therefore, this study employs the geodetic technique to monitor the deformation of the Sultan Idris Shah Bridge via the RTS.

### ***2.1.1 Geodetic monitoring survey technique***

Geodetic survey deformation monitoring techniques are able to produce absolute data and allow localised measuring devices, such as geotechnical instrumentation, to be connected together in a complementary way (Ogundare, 2016). Geodetic monitoring survey technique is a terrestrial base surveying method. It is usually based on the known point interconnected to each other by bearing and distance measurements to form a ground geodetic network. The technique merely monitors ground surface deformation and therefore provide an overall deformation trend of an object on the ground surface that is being monitored with respect to some stable reference control points. Table 1 show several instruments and equipment of geodetic monitoring.

**Table 1.** Geodetic Monitoring Instrument (Kalkan, Alkan, and Bilgi, 2010).

<b>Geodetic Methods</b>	<b>Instruments and Equipment</b>
Alignment Survey	Theodolite, Laser Optic, Invar wire
Conventional Survey	Theodolites and Electronic Distance Measurement Instrument (EDM)
Satellite Base Survey	GPS, GLONASS and GALILEO Receivers
Precise Trigonometric Levelling	Precise Theodolite and Precise EDM
Precise Geometric Levelling	Precise Levelling Equipment
Laser Scanning Technique	Laser Scanner
Interferometry SAR Image	Processing of SAR Image

### ***2.1.2 Non-geodetic monitoring survey***

Non-geodetic monitoring is a survey technique also known as geotechnical and structural surveying techniques (Ogundare, 2016). Non-geodetic monitoring surveys for deformation monitoring have the following characteristics as this technique can provide localise information at discrete locations with no physical correlation with another instrument. This technique can record parameters such as load, stress, deformation, pressure, tilting, and temperature regarding the structure under monitoring. The deformation behaviour of the structure being monitored, however, cannot be determined only by non-geodetic monitoring survey methods.

Furthermore, non-geodetic surveying does not provide redundant measurements. As a result, the resultant measurement is regarded as less reliable. The non-geodetic survey consists solely of repeated observations of the same observable, which may be deformed. As a result, unless compared with some other independent measurements, locally upsetting information is gained without any check.

There are certain advantages to using a non-geodetic survey technique, such as the fact that it is less labour intensive. The level of expertise necessary to operate a non-geodetic survey instrument is lower than that required to run a geodetic survey equipment. Besides that, non-geodetic survey techniques can sometimes yield high accuracy data within a few hundredths of a millimetre (0.01 mm). Table 2 show examples of non-geodetic monitoring instruments.

**Table 2.** Non-Geodetic Monitoring Instrument (Kalkan, Alkan, and Bilgi, 2010).

<b>Non-Geodetic Methods</b>	<b>Instruments</b>
Slope Measurement	Inclinometer
Displacement Measurement	Settlement Column
Length Change Measurement	Extensometer
Pore Water Measurement	Piezometer
Vertical displacement Measurement	Reversed Pendulum
Grouting Measurement	Joint Meter
Crack Measurement	Crack Meter

### **2.1.3 Control network**

Engineering structures such as bridges, building, and man-made structures build on the surface of the Earth will experience changes in its structural stability. Aside from all man-made features on the Earth's surface, the Earth's crust itself will endure deformations. These deformations must be measured, and the results must be gathered on a regular basis. As a consequence, absolute or relative geodetic control networks are established to obtain and collect measurements on deformable objects on a regular basis (Baryla et al., 2014; Chrzanowski and Chen, 1990; Nowel, 2015).

Absolute control networks are made up of monitoring points that are placed on the deformable object and reference points (or pillars) that are placed at a predetermined location that is usually far away from the deformable object and will not be affected by the effect of the factors that cause the deformable to deform. The mathematical stability of the reference points or pillar must be demonstrated.

In an absolute network, the coordinate of the reference point will be used to define the coordinate system (or the datum of the network); hence the reference pillars must be stable throughout the duration of the survey measurement epochs. Otherwise, the estimated deformation of the deformable item will be distorted if the network datum changes. Hence, in absolute network deformation analysis, the stability analysis of the reference pillars is very important (Amiri-Simkooei et al., 2017).

## 2.2 Determination of occupied observation station

In this study, the occupied observation station point coordinate is determined by using resection surveying method. The resection surveying method is also known as free stationing surveying (Grobler, 2016). Resection surveying is a control survey method, which extends the control station by establishing a new control point that is unknown coordinate from the known coordinate control point. The new unknown point can be coordinated by taking a measurement from the instrument set up on the unknown coordinate station without setting up the instrument on the known control point (Chukwuocha, 2018).

The major advantage of the resection survey is that the procedure is simple and can be easily carried out, especially for large surveying projects involving stacking out. The resection survey method also come in handy when coordinating points under a forest canopy where Global Positioning System (GPS) would not obtain a good result (Mackinnon & Murphy, 2011). The two-point resection method is illustrated in Figure 1.

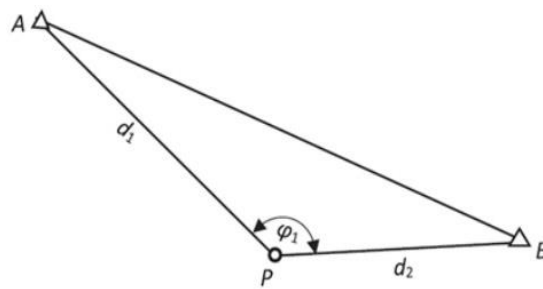


**Figure 1.** Two Point Resection Method

Referring to Figure 1, the known control points are A and B. The unknown point that needed to be coordinated is label as point P. The instrument is set up on point P. The internal angle APB is measured, as are the AP and BP. The angles of BAP and ABP can be computed using equation (1) below.

$$a^2 = b^2 + c^2 - 2bc \cos(A) \quad (1)$$

Then the azimuths for lines AP and BP are computed from the azimuth of the control line AB and using the angles BAP and ABP, respectively. After the azimuth and distance of AP and BP is computed, the coordinate of point P can be computed.

### 2.3 Coordinate time series graphs

The coordinate time-series graph is plotted using Matlab software. The calculation is shown as the equation (2) and (3) below:

$$\Delta dN_n = N_{\text{epoch } n} - N_{\text{ref}} \quad (2)$$

$$\Delta dE_n = E_{\text{epoch } n} - E_{\text{ref}} \quad (3)$$

The displacement of the Northing (N) and Easting (E) components are plotted against time (in second). Hence, a coordinate time series plot graph can be plotted. Each epoch's monitoring point reading is plotted. The time series depicts variations in the position of the monitoring point, which represent structural changes in the bridge. Following that, a functional model is chosen to fit a straight line or curve to a set of known coordinate points. Generally, the decision to employ a straight line, parabola, or other higher-order curve can be determined after charting the data by examining the magnitude of the residuals after solving for the least squares with the first line or curve selected.

To plot data into a displacement over time graph, the X-axis is the time, and the Y-axis represent the displacement. The data is then fitted into a straight line, as shown in Figure 2. The straight line can be represented by the equation (4):

$$y = mx + c \quad (4)$$

where y is a displacement,

m is a gradient of the graph =  $\frac{\text{difference in } y}{\text{difference in } x}$ ,

c is the y-intercept  $c = y\text{-intercept when } X=0$ ,

x= time.

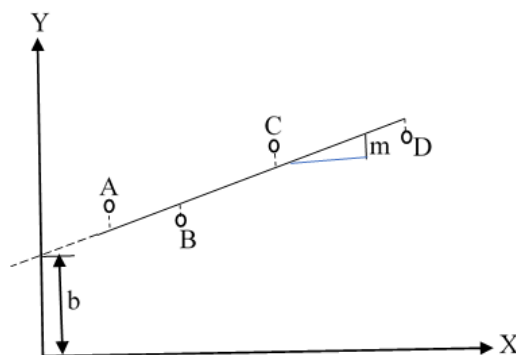


**Figure 2.** The data is fitted into a straight line

If the points were truly linear and there were no observational or experimental errors, all coordinates would lie on a straight line. However, this is rarely the case, and thus it is possible that the measured points may contain errors. If a line is selected as the model for the data, the equation of the best-fitting straight line is found by adding residuals to equation (5).

$$y + u_y = mx + c \quad (5)$$

For example:

$$y_A + u_{yA} = mx_A + b$$

$$y_B + u_{yB} = mx_B + b$$

$$y_C + u_{yC} = mx_C + b$$

$$y_D + u_{yD} = mx_D + b$$

Equation (5) contain two unknowns namely  $m$  and  $c$ ,  $u_y$  is the residuals. A matrix is from to solve the two unknowns. Their matrix representation is:

$$AX = L + V \quad (6)$$

Where designed matrix  $A = [x \ 1]$ ,

unknown parameters matrix,  $X = \begin{bmatrix} m \\ c \end{bmatrix}$ ,

observation value,  $L = [y]$ ,

residuals,  $V = [u_y]$ .

For example, there are four observations made. The observations are represented by the straight line, as shown in Table 3.

**Table 3.** Example of observations data

<b>x</b>	<b>y</b>
3.00	4.50
4.25	4.50
5.50	4.50
8.00	5.50



Represented by straight line equation:  $y + u_y = mx + c$

$$4.50 + u_{T1} = 3.00m + c$$

$$4.50 + u_{T2} = 4.25m + c$$

$$4.50 + u_{T3} = 5.50m + c$$

$$5.50 + u_{T4} = 8.00m + c$$

For example:

$$A = \begin{bmatrix} x_1 & 1 \\ x_2 & 1 \\ x_3 & 1 \\ x_4 & 1 \end{bmatrix}, \quad X = \begin{bmatrix} m \\ c \end{bmatrix}, \quad L = \begin{bmatrix} y_A \\ y_B \\ y_C \\ y_D \end{bmatrix}, \quad V = \begin{bmatrix} U_{T1} \\ U_{T2} \\ U_{T3} \\ U_{T4} \end{bmatrix}$$

rearrange become

$$\begin{bmatrix} 3.00 & 1 \\ 4.25 & 1 \\ 5.50 & 1 \\ 8.00 & 1 \end{bmatrix} \begin{bmatrix} m \\ c \end{bmatrix} = \begin{bmatrix} 4.50 \\ 4.50 \\ 4.50 \\ 5.50 \end{bmatrix} + \begin{bmatrix} U_{T1} \\ U_{T2} \\ U_{T3} \\ U_{T4} \end{bmatrix}$$

To form the normal equations, pre multiply matrices A and L by  $A^T$

$$\begin{bmatrix} 3.00 & 4.25 & 5.50 & 8.00 \\ 1 & 1 & 1 & 1 \end{bmatrix} \begin{bmatrix} 3.00 & 1 \\ 4.25 & 1 \\ 5.50 & 1 \\ 8.00 & 1 \end{bmatrix} \begin{bmatrix} m \\ c \end{bmatrix} = \begin{bmatrix} 3.00 & 4.25 & 5.50 & 8.00 \\ 1 & 1 & 1 & 1 \end{bmatrix} \begin{bmatrix} 4.50 \\ 4.50 \\ 4.50 \\ 5.50 \end{bmatrix} + \begin{bmatrix} U_{T1} \\ U_{T2} \\ U_{T3} \\ U_{T4} \end{bmatrix}$$

$$\begin{bmatrix} 121.3125 & 20.75 \\ 20.75 & 4.00 \end{bmatrix} \begin{bmatrix} m \\ c \end{bmatrix} = \begin{bmatrix} 105.8125 \\ 19.75 \end{bmatrix}$$

To form the normal equations, pre multiply matrices A and L by  $A^T$  and get for linear equation. Rearrange the equation to the following equation (7):

$$X = (A^T W A)^{-1} A^T W L \quad (7)$$

Where W is the weight matrix,

A is designed matrix,

X is unknown parameter,

L is observation value.

$$X = \begin{bmatrix} m \\ c \end{bmatrix} \begin{bmatrix} 121.3125 & 20.75 \\ 20.75 & 4.00 \end{bmatrix}^{-1} \begin{bmatrix} 105.8125 \\ 19.75 \end{bmatrix} = \begin{bmatrix} 0.246 \\ 3.663 \end{bmatrix}$$

Therefore,  $m = 0.246$  and  $c = 3.663$

Thus, the most probable values for  $m$  and  $c$  can be calculated. To obtain the residuals, the equation (8) is rearranged and solved as below. The residuals can be used to compute the standard deviation.

$$V = AX - L \tag{8}$$

$$V = \begin{bmatrix} V_1 \\ V_2 \\ \vdots \\ V_n \end{bmatrix}, \quad L = \begin{bmatrix} L_1 \\ L_2 \\ \vdots \\ L_n \end{bmatrix}, \quad \hat{X} = \begin{bmatrix} \hat{X}_1 \\ \hat{X}_2 \\ \vdots \\ \hat{X}_u \end{bmatrix}$$

$\uparrow$                        $\uparrow$                        $\uparrow$   
 Residual              Observation      Estimate Parameter

$$A = \begin{bmatrix} a_{11} & \cdots & a_{1u} \\ \vdots & \ddots & \vdots \\ a_{n1} & \cdots & a_{nu} \end{bmatrix} \quad \text{Designed matrix}$$

### 3. Methodology

This section describes the study area, instruments, activities in data acquisition and data processing. Figure 3 presents the research framework that has been applied.

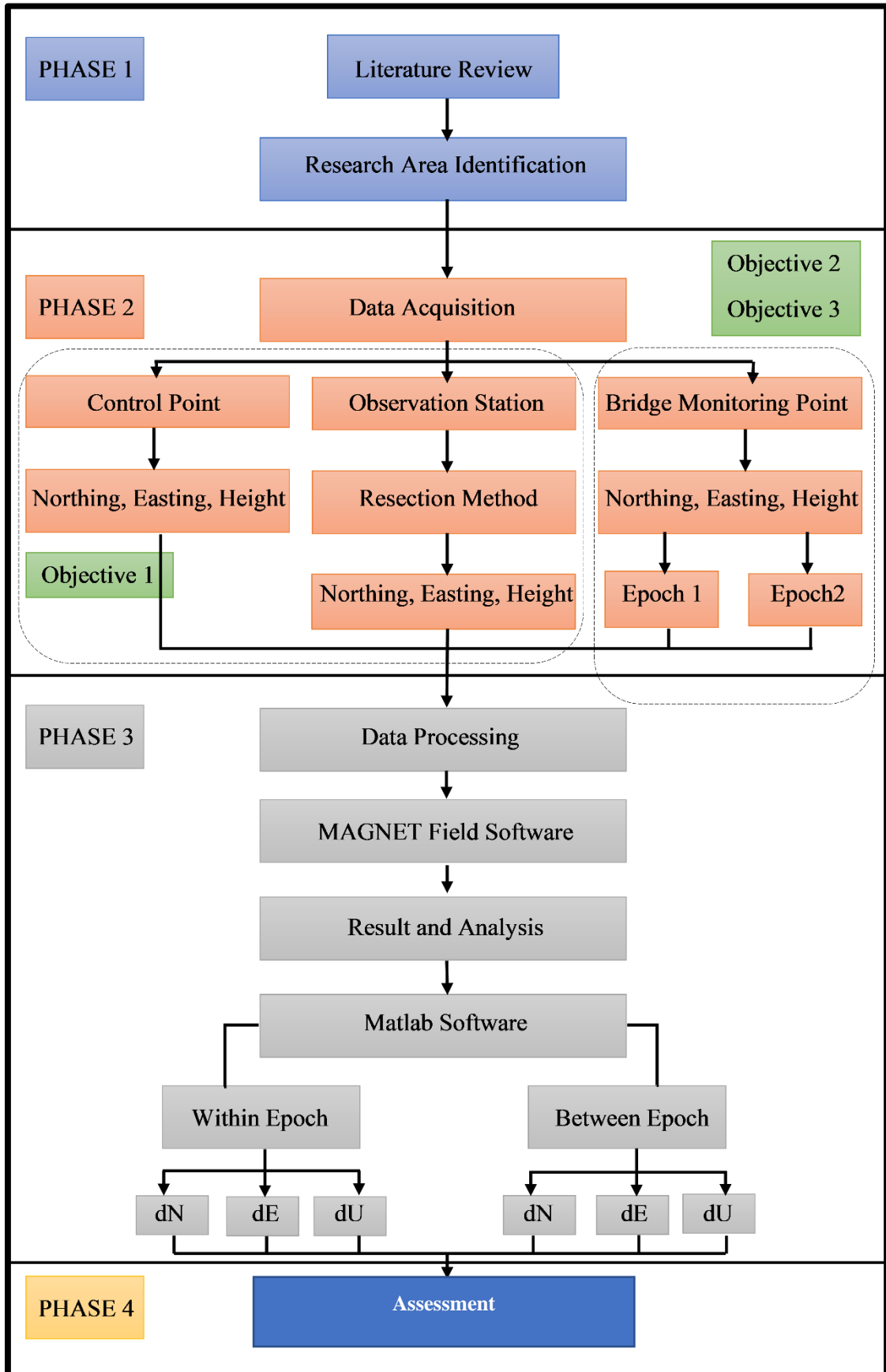


Figure 3. Research Methodology Framework

### ***3.1 Case Study***

As a case study, the Sultan Idris Shah Bridge in Ipoh, Perak was chosen. The Sultan Idris Shah Bridge connects Ipoh old town and Ipoh new town across the Kinta River and is one of the key bridges in Ipoh, Perak. Built in 1907, the Sultan Idris Shah Bridge has undergone periodic maintenance. This bridge connects Ipoh old town with Ipoh new town and is a major transit route used by locals on a daily basis. The Kinta River has a fast-moving river. Because of the history of the bridge, the amount of traffic it carries, and the strong river current that runs beneath it, it is believed that this bridge has deformed over time. Figure 4 shows the Sultan Idris Shah bridge, which is a six-column concrete bridge with a short span. The bridge has a 20-meter span, an 80-meter length, and a 20-meter width.



**Figure 4.** Sultan Idris Shah Bridge in Ipoh, Perak, Malaysia

### ***3.2 Instrumentation***

In this study, Topcon RTS GT-1001, as shown in Figure 5, is used as an instrument to carry out the structural monitoring of Sultan Idris Shah Bridge in Ipoh, Perak, Malaysia. The RTS instrument can provide automatic target detection and automatic monitoring function with high accuracy in an effective way. The instrument can obtain high accuracy and high precision point coordinate.



**Figure 5.** Topcon RTS GT-1001

The instrument comes with an automatic monitoring program function. A user just needs to key in the coordinate of the observation point, and the instrument can automatically perform monitoring work continuously. Suitable software to process and analyze the collected data such as Topcon Magnet Field software and Matlab software were explored.

### ***3.2 Data acquisition***

The second phase of the research methodology is data acquisition. The data acquisition is made at the Sultan Idris Shah Bridge in Ipoh, Perak, Malaysia. In this data acquisition, there are three items that need to be achieved and acquired. First, the base station, which acts as the 3-D control point has to be established. Three base points are established by using static observation using GPS equipment. The 3-D geographical coordinate obtained from the GPS equipment in the Geocentric Datum of Malaysia (GDM2000) is then projected to Geocentric Malayan Rectified Skew Orthomorphic (Peninsular Malaysia) onto a flat map (JUPEM, 2009).

A detailed procedure of base station (3-D control point) establishment by using GNSS is explained in section 3.2.1. Three occupied stations were constructed following the establishment of the three-dimensional control point. The three occupied stations will be converted into a monitoring station to monitor the bridge. The resection method is used to determine the coordinates of the occupied station. Section 3.2.2 details the approach for establishing an occupy station via the resection method.

Thirdly, monitoring locations will be established on the bridge. On the bridge, a total of ten target prisms will be put, five on the left and five on the right. The bridge was observed

from three separate occupied points. Section 3.2.3 details the technique for establishing monitoring sites. All established stations are depicted in Figure 6.



**Figure 6.** Position of Base Station, Occupy station and Monitoring Points.

### ***3.2.1 Establishment of base station***

The base station, which is the known point, is established using GNSS equipment. Static surveying technique was used to obtain the coordinate of the base station. Static surveying technique is a method of data collection where the point is observed for a duration of time, typically ranging from 30 minutes to few hours. A processing algorithm is employed to process the GNSS observation data to obtain the coordinate of the base point.

The processing software used to process the GNSS observation is Trimble Business Center. The raw data from the field observation are processed by this software. Network adjustment is applied to the final coordinate of the base point. Therefore, high accuracy and precision base station coordinate are obtained. The coordinate observed is a 3D coordinate system in the GDM2000 datum. The 3D coordinate was processed using a map projection module from Geocentric Datum of Malaysia GDM2000 to Geocentric Malayan Rectified Skew Orthomorphic (Peninsular Malaysia) (MRSO) onto a flat map (JUPEM, 2009).

### ***3.2.2 Establishment of occupy stations***

By using the method of resection, the location of the total station at occupy station can be determined by measuring the known points (Topcon, 2015). To obtain an unknown station's

coordinates, the unknown station must be visible to at least two controls; otherwise, the procedure fails. The calculation is solved by using the triangle form using the one unknown point and two known control points, which lines to two control stations and the included angle are measured without setting up the instrument on the control stations (Chukwuocha, 2018). Occupy stations 1, 2, and 3 were established by using two known base points (control points). Occupy station one was established with the assistance of base stations 1 and 3. The computation is solved by constructing a triangle from the three points, and the coordinates of the occupied station one may be determined. Occupy station 2 was established with the assistance of base stations 2 and 3. The calculation is solved by constructing a triangle from the three locations, and the coordinates of occupy station 2 may be computed. Occupy station 3 was constructed with the assistance of base stations 1 and 2. The computation is solved by constructing a triangle from the three locations, and the coordinates of the occupied station 3 can be determined.

The bridge has ten monitoring locations. Each side of the bridge has five monitoring sites. The bridge monitoring point must be tied directly to the bridge structure. During the observation, the monitoring stations must remain stationary. This is to guarantee that the monitoring point deformation is identical. Thus, by measuring the deformation of the monitoring point, the bridge deformation may be identified. Monitoring stations include reflector less, reflecting sheet, conventional prism, and 360 prism. Among all these monitoring locations, standard prism may provide the most accurate and precise measurement.

### ***3.2.3 Bridge monitoring data collection using topcon rts gt-1001***

The bridge's observation measurements were taken at three distinct occupied stations. To carry out the data collection and monitoring of the bridge, the monitoring point established on the bridge must be inter-visible with the occupied station. All obstructions in the way of clear vision must be removed. As shown in Figure 7, occupying station 1 (OCC1) monitored PT1000, PT2000, PT3000, PT4000, and PT5000 monitoring points, whereas occupying station 2 (OCC 2) monitored PT6000, PT7000, PT8000, PT9000, and PT10000 monitoring points.

Additionally, from occupy station 3 (OCC 3) , monitoring points for PT1000, PT2000, PT5000, PT6000, PT7000, and PT10000 were observed. Monitoring points on both sides of the bridge were observed and monitored at the same time from occupy station 3, with three monitoring points on the bridge's left side and three monitoring points on the bridge's right side.

In other words, occupy station 1 monitored the monitoring points on the right side of the bridge; occupy station 2 monitored the monitoring points on the left side of the bridge; while occupying station 3 monitored both sides of the bridge simultaneously in single epoch as illustrated in Figure 7.



**Figure 7.** Line of Sight from Occupy Station to Monitoring Points

The data acquisition entails two observational epochs separated by a three-month period. Epoch 1 took place in October 2019 and Epoch 2 took place in January 2020. Each monitoring session lasted about 2 hours in each period. In each epoch, the monitoring sites were measured for a total of 2 hours.

### ***3.3 Data processing***

In this stage, the data collected at the fieldwork were processed in the Topcon Magnet field software to compute the coordinate. Next, the data were further processed by using Matlab software, and the Coordinate Time Series (CTS) graph was plotted using Matlab software. The calculation is shown in equations (2) to (8).

From the Coordinate Time Series (CTS) graph, analysis of data was performed. The Matlab software was used to calculate site velocity estimation. The monitoring stations were monitored continuously over a period of approximately 2 hours; by comparing the coordinates, the changes in the displacement of the Northing and Easting components can be estimated. For monitoring point with the reference coordinate of monitoring points, the measured data were



stored in the MAGNET field software. The coordinate of the monitoring point was processed and exported in the form of coordinate data.

The RTS is set up at the occupied station (OCC 1, OCC 2 and OCC 3). The back-sight target is set on the GPS Basepoint (3-D control point). From the occupied station, the monitoring points were measured for a duration of approximately 2 hours in one epoch. The measurement is measured and recorded in horizontal azimuth, vertical angle, and distance. In the MAGNET field software, the data that are measured and recorded can be automatically computed into coordinate and height, which are Northing (in meter), Easting (in meter) and height (in meter). The data were then exported in bearing and distance formats.

The coordinate value computed by the MAGNET field software can be up to 6 decimal points. The high sensitivity in the computed coordinate is due to the ability of the RTS to measured 0.5" in angular measurement and 0.0001m in distance measurement. In this study, the coordinate of the monitoring points was exported to Matlab to analyse site velocity estimation.

#### **4. Result and discussions**

This section presents the equipment calibration test results, the analysis of coordinate of the base station, the stability of occupying station, the static model analysis to represent deformation of the concrete bridge and kinematic model analysis which is the plotting of coordinate time series graph to analyse the dynamic displacement over time of the Sultan Idris shah Bridge.

To ensure the used instrument measure reliable distances and obtain good relative coordinates on the surface of the Earth, the instrument has been calibrated at least once every six months for total station (or EDM) and at least once a year for the GNSS instrument. The equipment calibration test result is shown in Table 4.

**Table 4. EDM Calibration Result**

Pillar Number		Measured Distance, m	Horizontal Distance, m (A)	Known Distance, M (B)	Difference, m (A-B)
From	To				
1	2	94.9626	94.9626	94.96269	-0.00009
1	3	360.1355	360.1355	360.13935	-0.00385
1	4	710.1552	710.1552	710.16097	-0.00577
1	5	890.1270	890.1270	890.13245	-0.00545
1	6	900.1590	900.1590	900.16377	-0.00477
2	3	265.1723	265.1723	265.17713	-0.00483
2	4	615.1922	615.1922	615.19756	-0.00536
2	5	795.1641	795.1641	795.16992	-0.00582
2	6	805.1955	805.1955	805.20177	-0.00627
3	4	350.0200	350.0200	350.02015	-0.00015
3	5	529.9906	529.9906	529.99241	-0.00181
3	6	540.0232	540.0232	540.02422	-0.00102
4	5	179.9696	179.9696	179.97303	-0.00343
4	6	190.0033	190.0033	190.00445	-0.00115
5	6	10.0322	10.0322	10.03261	-0.00041
$\sum_1^n (A-B)$					-0.05018
$C = \frac{\sum_1^n (A-B)}{n}$					-0.00335

Where n = Number of observations

$$\text{Constant error, } C = \frac{\sum_1^n (A-B)}{n} \tag{9}$$

$$\text{Therefore, } C = \frac{\sum_1^n (-0.05018)}{15} = -0.00335 \text{ m}$$

From the calibration test result, the constant error of the Topcon RTS GT-1001 is -0.00335 m, which is below the maximum limit of constant error allowed that is 0.001m, according to JUPEM (2016). Hence, we conclude the instrument is in good condition.

#### **4.1 Establishment of base station and occupy station**

The coordinate of the base station is measured using GPS equipment static observation and processed using Trimble Business Centre (TBC) software. Table 5 shows the coordinates of three points.

**Table 5.** Coordinate of Base Stations in MRSO

<b>Points</b>	<b>Northing (m)</b>	<b>Easting (m)</b>	<b>Height (m)</b>
BASE 1	508902.70000000	343105.32300000	31.558
BASE 2	508961.52400000	343012.45400000	31.185
BASE 3	508843.38700000	343056.81500000	31.072

The coordinates of the Occupy Stations were determined using the resection approach from the coordinates of the base station (3-D control point). The accuracy and reliability of the occupied station are excellent. It is vital to test the stability and deformation resistance of the occupied station when building it. Table 6 shows the coordinates of the occupied station.

**Table 6.** Coordinate of Occupy Station Epoch 1

<b>Points</b>	<b>Northing (m)</b>	<b>Easting (m)</b>
OCC 1	508901.5936	343031.8664
OCC 2	508957.0607	343008.8503
OCC 3	508950.4962	342988.3133

##### **4.1.1 Occupy station stability analysis**

An absolute network for deformation analysis is used in this monitoring survey, which is a control network designed to establish by using these occupy stations. The coordinate of the occupied station has been used to define the coordinate system or the datum of the network.

The stability analysis for occupy station was carried out before the start of work in epoch 2. It is very important to carry out stability analysis in an absolute network because the instability of occupy station will cause changes in the coordinate system or datum of the network. Otherwise, the estimated deformation of the deformable object will be distorted because there are changes in the network coordinate system or network datum.

In epoch 2, the coordinate of the occupy station were resurvey using close loop traverse method. The traversing method is a method of control surveying and is used to determine the coordinate of the occupied station (Harvey, 2012). From the result of the travel, the coordinate of the occupied station is shown in Table 7.

**Table 7.** Coordinate of Occupy Station Epoch 2

Points	Northing (m)	Easting (m)
OCC 1	508901.5911	343031.8686
OCC 2	508957.0627	343008.8471
OCC 3	508950.5032	342988.3144

The difference in the geometrical displacement of occupying station between epoch 1 and epoch 2 is shown in Table 8.

**Table 8.** Geometrical Displacement of Occupy Station between Epoch1 and Epoch 2 in three months duration

Points	$\Delta$ Northing (m)	$\Delta$ Easting (m)	Magnitude (m)	Azimuth
OCC 1	0.0025	-0.0022	0.0034	140°07'34.92"
OCC 2	-0.0020	0.0032	0.0038	306°54'13.32"
OCC 3	-0.0070	-0.0011	0.0070	8°57'56.88"

The greater the magnitude of the displacement vector, the less stable the station. From the stability analysis, the displacement of occupy station is under the acceptable range. Figure 8 visualised the geometrical displacement of occupy station between 2 epochs.

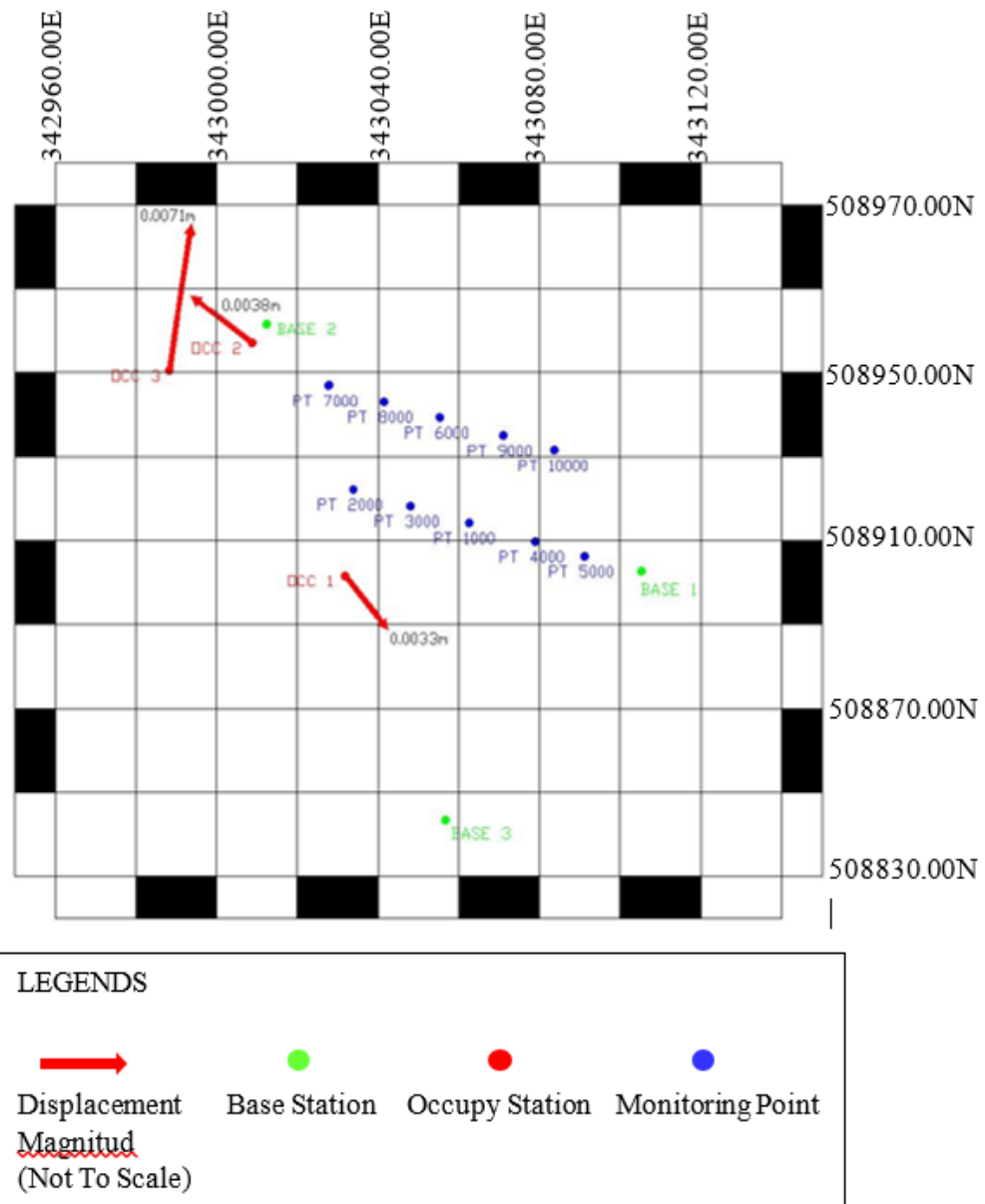


**Figure 8.** Vector Plot Map Visualise Geometrical Displacement of Occupy Station between 2 Epochs

#### 4.1.2 Bridge monitoring

The RTS is installed on each occupied station, and the geometrical position of the monitoring sites is measured and recorded. Typically, measurements are done on a restricted number of monitoring points that are correctly established in key positions to extrapolate the behaviour of the entire structure and quantify the absolute or relative deformation of the structure (Scaioni et al., 2018). When performing deformation analysis of a structure, there are different type of

modelling method can be used to model the deformation. Different types of modelling methods can be employed to model the deformation of a structure when performing a deformation study. There are numerous types of deformation models; one of them is a static model, or basic model, which is independent of time and causative forces. The examination is limited to the presence or absence of deformity. The static model's primary purpose is to determine the amount and significance of movements. The method of deformation monitoring modelling may be used to analyse a long-term pattern (Pytharouli et al., 2007; Wieland and Kirchen, 2012) or to follow a specific event, such as an earthquake (Radhakrishnan, 2006). The difference in the geometrical displacement of monitoring points between epoch 1 and epoch 2 is shown in Table 9.

**Table 9.** Geometrical Displacement of Monitoring Points between Epoch1 and Epoch 2 in three months duration

<b>Points</b>	<b>ΔNorthing (m)</b>	<b>ΔEasting (m)</b>	<b>Magnitude (m)</b>	<b>Azimuth</b>
1000	0.0020	-0.0009	0.0022	335°49'37.08"
2000	-0.0352	-0.0033	0.0354	185°21'20.87"
3000	-0.0191	-0.0193	0.0272	223°53'09.94"
4000	-0.0140	-0.0315	0.0345	236°02'12.37"
5000	-0.0060	-0.0315	0.0321	237°17'33.45"
6000	0.0147	0.0005	0.0147	1°56'53.10"
7000	0.0254	-0.0331	0.0417	310°34'50.05"
8000	0.0137	0.0004	0.0137	1°40'20.62"
9000	0.0339	-0.0273	0.0435	321°47'02.46"
10000	0.0332	-0.0193	0.0384	329°59'53.97"

Measurements are taken multiple times, and the results are utilised to generate the error ellipse with a 95% confidence level. The points are considered to be deformed if the magnitude of the geometrical displacement is greater than the error ellipse. The error ellipse of the ten monitoring points is depicted in Figure 9. Table 10 summarises the results of the error ellipse.

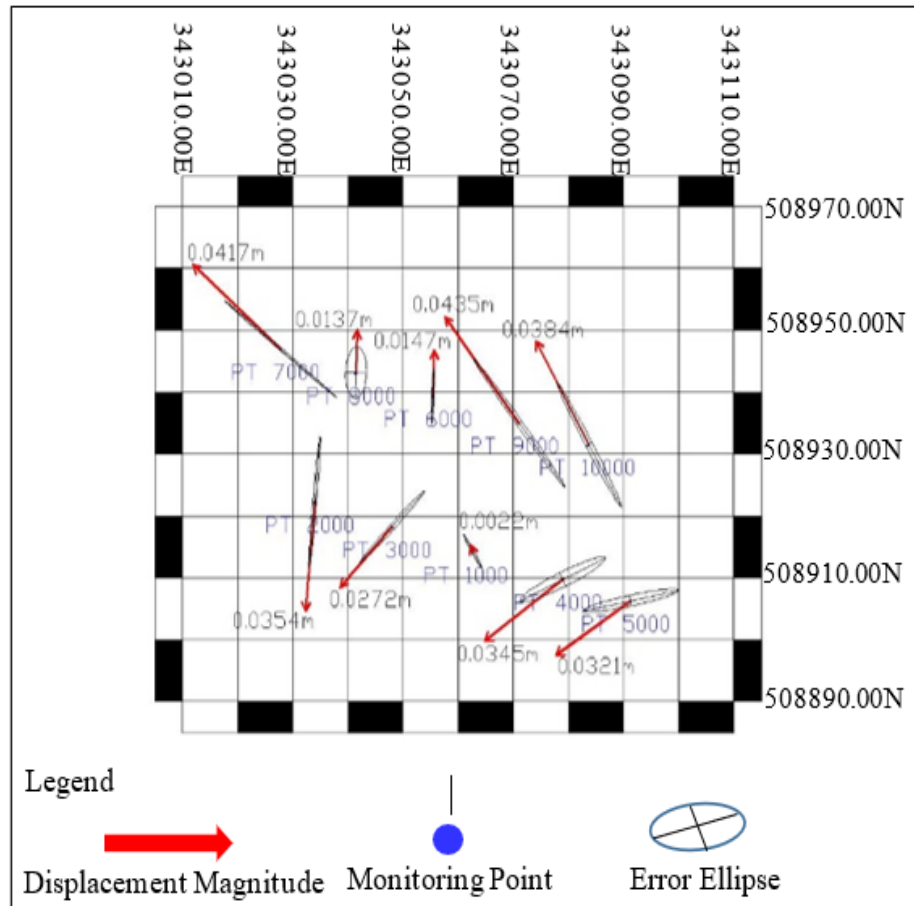


**Figure 9.** Error Ellipse of Monitoring Points

Only the PT1000 geometrical displacement is within the error ellipse, as shown in table 10 and figure 9. The geometrical displacement of all nine remaining monitoring locations exceeds the error ellipse. The direction of displacement of the left side of the bridge is towards the south-west direction, and the left side of the bridge is moving towards the north-west direction, according to the vector plot. As a result, the premise of the Sultan Idris Shah bridge's vulnerability is supported.

The next type of modelling is a kinematic model where it involves a time-dependent function but is independent of causative forces. The purpose of the kinematic model is to study the spatial characteristics of deformation and its temporal attributes. It also examined the motion of network points and described velocity and acceleration. The observation of dynamic movements of the deformable object requires high-frequency sensors (García-Palacios et al., 2016) that are able to continuously track accelerations (Altunişik et al., 2016; Lienhart, Ehrhart, and Grick, 2017) at specific points. RTS can acquire measurement accurately and fast; it is

suitable to perform a kinematic model of deformation analysis, which can continuously track accelerations of specific points (Altunışık et al., 2016; Lienhart, Ehrhart, and Grick, 2017). Table 11 shows the site velocity and range of displacement for the northing and easting components in two hours.

**Table 10.** Error Ellipse of Monitoring Points

<b>Point</b>	<b><math>\sigma</math> Northin g (m)</b>	<b><math>\sigma</math> Easting (m)</b>	<b>Semi Major Axis (m)</b>	<b>Semi Minor Axis (m)</b>	<b>Azimuth</b>
1000	0.0044	0.0027	0.0127	0.0010	148°34'46"
2000	0.0174	0.0017	0.0428	0.0013	5°23'06"
3000	0.0095	0.0096	0.0329	0.0019	45°18'30"
4000	0.0060	0.0127	0.0340	0.0048	65°50'43"
5000	0.0031	0.0142	0.0355	0.0034	79°02'35"
6000	0.0074	0.0005	0.0180	0.0008	2°24'04"
7000	0.0127	0.0165	0.0508	0.0009	127°30'58"
8000	0.0069	0.0031	0.0168	0.0076	2°34'48"
9000	0.0169	0.0136	0.0531	0.0022	141°18'20"
10000	0.0166	0.0096	0.0468	0.0025	149°59'23"

The range of displacement of the data and the trend of the data does not satisfy the requirement, according to the observations made. The Topcon RTS GT-1001 is not capable of collecting high-frequency data. As a result, the kinematic model analysis is unsatisfactory.



**Table 11.** Site Velocity and range of displacement for Northing and Easting Component in two hours duration

Point	Component	Displacement over time (mm/s)	Range of displacement (mm)
<b>Epoch 1</b>			
PT1000	Northing	0.002337	18.0862
	Easting	0.001409	11.3487
PT2000	Northing	-1.78E-05	0.8524
	Easting	1.99E-04	3.1496
PT3000	Northing	-1.76E-04	2.6083
	Easting	1.44E-04	2.3011
PT4000	Northing	-4.38E-04	7.846
	Easting	6.42E-05	1.6623
PT5000	Northing	-0.002069	8.3321
	Easting	1.13E-04	1.5891
PT6000	Northing	-3.28E-04	2.9602
	Easting	-1.67E-04	1.6534
PT7000	Northing	-9.98E-05	1.1864
	Easting	-1.01E-04	1.1248
PT8000	Northing	-4.93E-04	3.068
	Easting	-2.33E-04	1.3673
PT9000	Northing	-4.77E-04	3.6115
	Easting	-1.88E-04	1.5898
PT10000	Northing	-5.16E-04	5.914
	Easting	-2.09E-04	2.2644
<b>Epoch 2</b>			
PT1000	Northing	-8.40E-05	1.1224
	Easting	1.73E-05	0.6502
PT2000	Northing	-1.14E-05	0.7256
	Easting	1.80E-05	0.6692
PT3000	Northing	9.42E-05	2.2541
	Easting	-8.08E-05	2.1034

PT4000	Northing	-6.93E-04	7.7098
	Easting	1.09E-04	3.3832
PT5000	Northing	7.36E-05	2.5821
	Easting	5.23E-05	0.9934
PT6000	Northing	2.39E-04	4.987
	Easting	1.10E-04	2.0075
PT7000	Northing	8.28E-05	2.0821
	Easting	6.06E-05	1.2023
PT8000	Northing	1.40E-04	3.4607
	Easting	7.56E-05	1.501
PT9000	Northing	2.80E-04	5.5162
	Easting	1.23E-04	2.1519
PT10000	Northing	3.24E-04	6.8891
	Easting	1.83E-04	2.9586

## 5. Conclusion

This study concludes that the Sultan Idris Shah Bridge deforms between 1.3 cm and 4.2 cm. The Topcon GT-1001 Robotic Total Station can perform deformation monitoring with centimetre level accuracy. Monitoring locations on the bridge's left side experienced deformation in a south-west direction, whereas monitoring stations on the bridge's right side experienced deformation in a north-west direction. Therefore, RTS is a viable method for monitoring bridge deformation, not just for static modelling, but also for dynamic monitoring of the bridge's vibration and displacement. Nevertheless, this study discovered that the RTS has several limitations when used with a kinematic model of deformation analysis. To begin, the Topcon RTS GT-1001's sampling rate is quite low. Due to the low sampling rate, the data acquired is sparse and therefore cannot be used to represent the network point's actual motion. Additionally, the RTS has difficulty tracking minor and quick movements, such as the shaking of a bridge when a huge and heavy car passes over it. The third shortcoming of the RTS is that it does not always point straight to the prism's centre, as demonstrated in Chua's experiment (2004). However, when distance variations are taken into account, contemporary RTS have significantly improved measurement accuracy with the addition of updated time of flight EDM

units (see Lackner and Lienhart, 2016). The RTS approach has been introduced as a substitute for structural monitoring. The RTS may be used to determine the bridge's geometrical position displacement deformation, which can be utilised to determine the bridge's and other structures' structural health. To monitor a structure dynamically, a high sample rate RTS is required. The outcome of the RTS-measured observation data can be utilised to determine the efficacy, applicability, and accuracy of structural monitoring. The findings suggest a technique for future monitoring efforts. It serves as a guide and source of information for future scholars interested in learning more about the application of RTS in structural monitoring.

Some recommendations are suggested to enhance the study such as (i) to use a higher sampling rate RTS to perform dynamic monitoring of the geometrical position of the bridge, (ii) to use concrete pillar as the occupy station instead of a tripod to ensure more excellent station stability, (iii) to observe the monitoring point from multiple occupy station to perform Least Square Adjustment of the network, (iv) to perform precise levelling to obtain the geometrical displacement of the vertical component of the bridge and (v) lastly to perform analysis using relative control network for the deformation monitoring of the bridge.

### **Acknowledgement**

The authors would like to thank to Makmal Ukur Kejuruteraan dan Kadaster (UKK) for providing instrumentation for this study. Special thanks to Dewan Bandaraya Ipoh for giving the permission to conduct the research at Sultan Idris Shah bridge. This research is financially supported by the Malaysia Ministry of Higher Education and Universiti Teknologi Malaysia, where research work is part of Tier 1 Universiti Teknologi Malaysia Research Grant (No. Q.J130000.2527.13H04).

## References

- Abdullahi, I.M. and Yelwa, N.A., 2016. "Structural Deformation Monitoring Surveys of New Administrative Building of Federal School of Surveying, Oyo–Nigeria". *International Journal of Science and Technology*, 6(1):1-14.
- Altunişik, A.C., Günaydin, M., Sevim, B., Bayraktar, A. and Adanur, S., 2016. "Retrofitting Effect on the Dynamic Properties of Model-Arch Dam with and Without Reservoir Water Using Ambient-Vibration Test Methods". *Journal of Structural Engineering*, 142(10) :04016069.
- Amiri-Simkooei, A.R., Alaei-Tabatabaei, S.M., Zangeneh-Nejad, F. and Voosoghi, B., 2017. "Stability Analysis of Deformation-Monitoring Network Points Using Simultaneous Observation Adjustment of Two Epochs". *Journal of Surveying Engineering*, 143(1) :04016020.
- Baryla, R., Paziewski, J., Wielgosz, P., Stepniak, K. and Krukowska, M., 2014. "Accuracy Assessment of the Ground Deformation Monitoring with the Use of GPS Local Network". Open Pit Mine Koźmin Case Study. *Acta Geodynamica et Geomaterialia*, 11(4), :176.
- Chen, Z.Q., Zheng, S.X., Zhou, Q., Chen, Z.W. and Li, X., 2020. "Extreme Value Distribution and Dynamic Reliability Estimation of High-Pier Bridges Subjected to Near-Fault Impulsive Ground Motions". *Advances in Structural Engineering*, 23(7):1367-1382.
- Chrzanowski, A., & Chen, Y. (1990). *Deformation monitoring, analysis, and prediction-status report*. Paper presented at the FIG XIX Congress, Helsinki.
- Chua, C. S. (2004). "Testing of Robotic Total Stations for Dynamic Tracking". *Undergraduate Thesis. Faculty of Engineering and Surveying, University of Southern Queensland*.
- Chukwuocha, A.C., 2018. "Using Reorientation Traversing on A Single-Unknown Station or Multiple-Unknown Stations to Solve the Two-Point Resection (Free Station) Problem". *Surveying and Land Information Science*, 77(1) :45-54.
- Cosser, E., Roberts, G.W., Meng, X. and Dodson, A.H., 2003, May. "Measuring the Dynamic Deformation of Bridges Using A Total Station". In *Proceedings of the 11th FIG Symposium on Deformation Measurements, Santorini, Greece* ,Vol. 25.
- Erol, S., Erol, B. and Ayan, T., 2004, July. "A General Review of the Deformation Monitoring Techniques and A Case Study: Analysing Deformations Using GPS/Levelling" In *Xxth ISPRS Congress*, Vol. 7 (No. 5) :12).

- Gaglione, A., Rodenas-Herreraiz, D., Jia, Y., Nawaz, S., Arroyo, E., Mascolo, C., Soga, K. and Seshia, A.A., 2018. *"Energy Neutral Operation of Vibration Energy-Harvesting Sensor Networks for Bridge Applications"*.
- García-Palacios, J.H., Soria, J.M., Díaz, I.M. and Tirado-Andrés, F., 2016, September. *"Ambient Modal Testing of A Double-Arch Dam: The Experimental Campaign and Model Updating"*. In *Journal of Physics: Conference Series* , Vol. 744, (No. 1) :012037. IOP Publishing.
- Grobler, H., 2016. *"Does the Underground Sidewall Station Survey Method Meet MSHA Standards?"*. *South African Journal of Geomatics*, 5(2) :175-185.
- Harvey, B.R., 2012. *"Survey Computations"*. *Surveying & Geospatial Engineering*, The University of New South Wales, Sydney.
- Kalkan, Y., Alkan, R. M., & Bilgi, S. (2010). *"Deformation Monitoring Studies at Atatürk Dam"*.
- Khodabandehlou, H., Pekcan, G. and Fadali, M.S., 2019. *"Vibration-Based Structural Condition Assessment Using Convolution Neural Networks"*. *Structural Control and Health Monitoring*, 26(2) :2308.
- King, N.S. and Malaysia, P.W.D., 1999. *"Malaysian Bridges-Status and Condition"*. Lecture Notes for Special Course on Bridge Assessment and Rehabilitation, Civil Engineering Department. Universiti Putra Malaysia :2-4.
- Lienhart, W., Ehrhart, M., & Grick, M. (2017). *"High Frequent Total Station Measurements for the Monitoring of Bridge Vibrations"*. *Journal of Applied Geodesy*, 11(1) :1-8.
- Lackner, S. and Lienhart, W., 2016, March. *"Impact of Prism Type and Prism Orientation on The Accuracy of Automated Total Station Measurements"*. In *Proceeding the 3rd Joint International Symposium on Deformation Monitoring*.
- Masreta Mohd, Othman Zainon, Zulkifli Majid and Abdul Wahid Rasib (2021). *Damage Inspection on Pier of Sg. Perak Reservoir Bridge Using Accelerometer and GNSS*. International Conference. GBES 2021 Universiti Teknologi Malaysia, Johor Bahru. Johor (22-23<sup>th</sup> June 2021)
- Nowel, K., 2015. *"Robust M-Estimation in Analysis of Control Network Deformations: Classical and New Method"*. *Journal of Surveying Engineering*, 141(4) :04015002.
- Ogundare, J.O., 2015. *"Precision Surveying: The Principles and Geomatics Practice"*. John Wiley & Sons
- Palazzo, D., Friedmann, R., Nadal, C., Santos, F.M., Veiga, L. and Faggion, P., 2006, October.

- "Dynamic Monitoring of Structures Using A Robotic Total Station"*. In Proceedings of the Shaping the Change XXIII FIG Congress, Munich, Germany, Vol. 813.
- Pytharouli, S., Kontogianni, V., Psimoulis, P., Nickitopoulou, A., Stiros, S., Skourtis, C., Stremmenos, F. and Kountouris, A., 2007. *"Geodetic Monitoring of Earthfill and Concrete Dams in Greece"*. International Journal on Hydropower and Dams, 14(2) :82.
- Radhakrishnan, N., 2006, May. "Direct GPS Measurement of Koyna Dam Deformation During Earthquake. In Proceedings of The 3rd IAG/12th FIG Symposium, Baden, Austria :22-24.
- Scaioni, M., Marsella, M., Crosetto, M., Tornatore, V. and Wang, J., 2018. *"Geodetic and Remote-Sensing Sensors for Dam Deformation Monitoring"*. Sensors, 18(11) :3682.
- Wieland, M. and Kirchen, G.F., 2012. *"Long-Term Dam Safety Monitoring of Punt Dal Gall Arch Dam in Switzerland"*. Frontiers of Structural and Civil Engineering, 6(1), :76-83.
- Yu, J., Zhu, P., Xu, B. and Meng, X., 2017. *"Experimental Assessment of High Sampling-Rate Robotic Total Station for Monitoring Bridge Dynamic Responses"*. Measurement, 104, :60-69.